NASA TECHNICAL NOTE

NASA TN D-2343

NASA TN D-2343

THE CAPABILITY OF A PROPORTIONAL-TYPE LATERAL CONTROL SYSTEM IN PROVIDING AERODYNAMIC HEADING-ANGLE TRAJECTORY CONTROL DURING REENTRY

by Gene W. Sparrow

Langley Research Center
Langley Station, Hampton, Va.

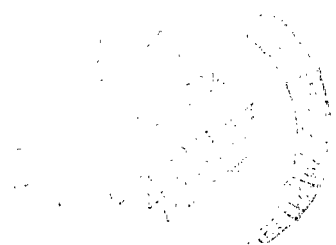NATIONAL AERONAUTICS AND SPACE ADMINISTRATION • WASHINGTON, D. C. • JULY 1964

THE CAPABILITY OF A PROPORTIONAL-TYPE LATERAL CONTROL SYSTEM IN PROVIDING AERODYNAMIC HEADING-ANGLE TRAJECTORY CONTROL DURING REENTRY

By Gene W. Sparrow

Langley Research Center
Langley Station, Hampton, Va.

NATIONAL AERONAUTICS AND SPACE ADMINISTRATION

THE CAPABILITY OF A PROPORTIONAL-TYPE LATERAL CONTROL

SYSTEM IN PROVIDING AERODYNAMIC HEADING-ANGLE

TRAJECTORY CONTROL DURING REENTRY

By Gene W. Sparrow
Langley Research Center

SUMMARY

An analog investigation has been made to determine the capability of a proportional-type lateral control system of providing aerodynamic heading-angle control of a vehicle having a maximum lift-drag ratio of 2.0 during reentry into the earth's atmosphere. Heading-angle changes were accomplished by means of a heading-angle-command step input to control equations which caused the vehicle to assume a roll attitude. Both roll and Dutch roll damping were augmented. The investigation was conducted at altitudes of 100,000, 150,000, and 210,000 feet. Control-system gains were varied at each of these flight conditions in an effort to determine the effects of these gains on the vehicle response. Results indicate that a sideslip-rate damper was superior to a yaw-rate damper in minimizing the magnitude of sideslip angle during roll. Though it was found necessary to adjust control-system gains at each flight condition for the most desirable vehicle response (minimum sideslip, rapid heading-angle response), results indicate that a partial relaxation of these desirable responses could simplify the system with the result that only one of the many control-system gains, the roll damper gain, need be varied with flight condition.

INTRODUCTION

Considerable research has been conducted on the problem of controlling and guiding a reentry vehicle from the fringes of the earth's atmosphere to a landing on the earth. Results of these investigations have resulted in defining a "footprint," or an accessible landing area which is subject to initial conditions and restraints (such as aerodynamic heating and accelerations) of the reentry vehicle. Basically, research has been concerned with controlling the trajectory of the reentry vehicle by way of treating the vehicle as a particle subject to aerodynamic lift, drag, and side forces (see refs. 1 to 4) with little attention being given to the dynamics of the vehicle necessary to provide trajectory control.

In the present paper the problem of providing lateral control to produce lateral range capability during reentry is considered. A proportional-type lateral control system is utilized, which provides lateral range capability by

producing a wind-heading-angle change by means of banking the vehicle in response to a step input of wind-heading-angle command. An analog investigation of the problem was conducted, and results presented show the effects of control-system gains, heading- and bank-angle inputs, and yaw- and sideslip-rate dampers on the vehicle response and stability over a range of flight conditions from 210,000 to 100,000 feet. Results are presented as time histories.

SYMBOLS

b wing span, ft

C_L lift-force coefficient

C_l rolling-moment coefficient, $\dfrac{\text{Rolling moment}}{qSb}$

$$C_{l_p} = \frac{\partial C_l}{\partial\left(\dfrac{pb}{2V}\right)}$$

$$C_{l_\beta} = \frac{\partial C_l}{\partial\beta}$$

$$C_{l_{\delta_a}} = \frac{\partial C_l}{\partial\delta_a}$$

C_n yawing-moment coefficient, $\dfrac{\text{Yawing moment}}{qSb}$

$$C_{n_r} = \frac{\partial C_n}{\partial\left(\dfrac{rb}{2V}\right)}$$

$$C_{n_\beta} = \frac{\partial C_n}{\partial\beta}$$

$$C_{n_{\delta_a}} = \frac{\partial C_n}{\partial\delta_a}$$

$$C_{n_{\delta_r}} = \frac{\partial C_n}{\partial\delta_r}$$

C_Y side-force coefficient, $\dfrac{\text{Side force}}{qS}$

$$C_{Y_\beta} = \frac{\partial C_Y}{\partial \beta}$$

D   drag force, lb

$F_{s,X}, F_{s,Y}, F_{s,Z}$ forces along X_s-, Y_s-, and Z_s-axes, lb

$F_{w,X}, F_{w,Y}, F_{w,Z}$.   forces along X_w-, Y_w-, and Z_w-axes, lb

g   acceleration due to gravity, 32.2 ft/sec^2

h   altitude, ft

I_X moment of inertia about X-axis, slug-ft^2

I_Z moment of inertia about Z-axis, slug-ft^2

K_1, K_2, K_3, K_4, K_5 control-system gains

L   lift force, lb

L/D   lift-drag ratio

$(L/D)_{max}$ maximum value of L/D

m   mass of vehicle, slugs

M   Mach number

p   roll rate about X-axis, radians/sec

q   dynamic pressure, lb/sq ft

Q_w force term defined in appendix

r   yaw rate about Z-axis, radians/sec

R_w force term defined in appendix

S   wing area, sq ft

t   time, sec

V   velocity, ft/sec

X,Y,Z   body axes

X_s, Y_s, Z_s stability axes

X_w, Y_w, Z_w wind axes

Y side force, lb

α angle of attack

β angle of sideslip

γ flight-path angle

δ_a aileron deflection

$\delta_a{}'$ aileron deflection as defined by control equation (2)

δ_r rudder deflection

$\delta_r{}'$ rudder deflection as defined by damper equation (3)

ϕ_c command bank angle

$\phi_c{}'$ command bank angle as defined by control equation (1)

ψ, θ, ϕ body-axis Euler angles

ψ_w, θ_w, ϕ_w wind-axis Euler angles

$\psi_{w,c}$ command wind-axis heading angle

ϵ_ϕ bank-angle error

$\epsilon_{\psi,w}$ wind-axis heading-angle error

    Dots above quantity denote differentiation with respect to time. All
angles are in radians unless otherwise noted.

ANALYSIS

Scope of Problem

    The investigation of the problems of providing lateral vehicle control
during reentry was conducted by way of analyzing the vehicle lateral response
characteristics at several discrete points along a typical reentry trajectory
by means of linearized equations of motion. Three flight conditions of alti-
tudes 100,000, 150,000, and 210,000 feet representing a range of flight environ-
ments were chosen for the investigation from the trajectory of a reentry vehicle
descending in an unbanked attitude at a constant angle of attack of 25° from
nearly circular orbital conditions at 380,000 feet to an altitude of
100,000 feet. The flight-path angle was initially at 0°. Although all aero-
dynamic and trajectory parameters were held constant during an investigation at

a particular flight condition, results obtained were assumed to be valid since the duration of a particular investigation was held to less than a minute of real time. Control-system gains were selected and adjusted empirically in a prescribed order (to be subsequently described) at each flight condition on the basis of observed vehicle responses.

Control System

Control-system description.- The block diagram of the lateral control system used in the investigation is shown in figure 1. Prior to a step input to the control system, the reentry vehicle was assumed to be in straight and level flight. A command wind-axis heading angle $\psi_{w,c}$, subsequently referred to as command-heading angle, serves as input to the control system and together with heading-angle ψ_w and heading-rate $\dot{\psi}_w$ feedbacks form the mathematical control equation

$$\phi_c' = K_1(\psi_{w,c} - \psi_w) - K_2\dot{\psi}_w \tag{1}$$

commanding a body bank-angle attitude ϕ_c'. Control-system gains K_1 and K_2 are, respectively, heading-error and heading-rate gains. The command bank angle ϕ_c is limited to $\pm 45°$, a value that will yield maximum lateral range for small heading-angle change and small flight-path angle. (See ref. 2.)

The command bank angle serves as input to the bank command loop of the control system and together with bank-angle ϕ and bank-angle-rate $\dot{\phi}$ feedbacks form the second mathematical control equation

$$\delta_a' = K_3(\phi_c - \phi) - K_4\dot{\phi} \tag{2}$$

which commands the aileron deflection δ_a'. Control-system gains K_3 and K_4 are, respectively, bank-angle-error and roll-rate gains. The aileron-control deflection is limited to $\pm 30°$.

The aileron and rudder (δ_r) deflections serve as inputs to the vehicle lateral equations of motion (see section entitled Vehicle and Equations of Motion) and result in an output of bank angle. The rudder control was limited to $\pm 30°$ and provided damping in yaw or sideslip through the damper equations

or

$$\left.\begin{aligned} \delta_r' &= K_5 r \\[2em] \delta_r' &= -K_5\dot{\beta} \end{aligned}\right\} \tag{3}$$

5

where r and $\dot{\beta}$ are, respectively, yaw and sideslip rates. The third control equation

$$\psi_w = \frac{0.906L}{mV} \int_0^t \sin \phi \; dt \qquad (4)$$

generates heading angle from the Euler body-axis angle ϕ. Equation (4) is an approximate expression based upon an assumed coordinated turn maneuver and was derived from reference 5. The derivation of equation (4) is given in the Appendix.

Selection of control-system gains.- Control-system gains K_1, K_4, and K_5 were selected at each flight condition on the basis of observed vehicle responses and in a prescribed order described in the following paragraph. On the basis of a preliminary investigation it was found that gains K_2 and K_3 could be held constant over the complete flight region with adequate control of the vehicle being provided with the remaining control-system gains. The values of K_2 and K_3 chosen were 50 and 23, respectively.

In selecting control-system gains at a given flight condition, the bank-angle command loop (fig. 1) was first considered independently of the complete control system. A step input of $\phi_c = 45^\circ$ was used as input to the bank command loop since it represented the maximum value of ϕ_c that could be generated by the outer loop. Control-system gain K_4 was then selected to provide a roll response on the verge of overshooting the command bank attitude. It was believed that the utilization of this easily observed roll criteria resulted in a satisfactory rapid well-damped roll response. A yaw damper was used to provide oscillatory stability of the vehicle during the rolling maneuver. Following the selection of K_4 the effects of yaw and sideslip dampers on the control system were examined and a damper gain K_5 was selected. Roll damper gain K_4 was subsequently adjusted to correct for the effect of gain K_5. For the complete control system, the bank command loop gains (K_3, K_4, K_5) were held constant and the gain K_1 was varied to provide satisfactory heading-angle response for a range of heading-angle-command step inputs. This sequence of selecting control-system gains was repeated at each flight condition.

Vehicle and Equations of Motion

The reentry vehicle used in this investigation has a maximum L/D capability of 2. The physical and inertial characteristics of the reentry vehicle are as follows:

m, slugs 310
S, sq ft 400
b, ft 20.7
I_X, slug-ft^2 3,950
I_Z, slug-ft^2 17,300

The equations of motion that define the vehicle lateral degrees of freedom in the body-axis system are as follows:

$$\left.\begin{array}{l} \dfrac{I_X}{qSb}\ \dot{p} = \dfrac{bC_{l_p}}{2V}\ p + C_{l_\beta}\beta + C_{l_{\delta_a}}\delta_a \\[3mm] \dfrac{I_Z}{qSb}\ \dot{r} = \dfrac{bC_{n_r}}{2V}\ r + C_{n_\beta}\beta + C_{n_{\delta_r}}\delta_r + C_{n_{\delta_a}}\delta_a \\[3mm] \dot{\beta} = -r\cos\alpha + p\sin\alpha + \dfrac{qS}{mV}\ C_{Y_\beta}\beta \end{array}\right\} \qquad (5)$$

Since small angle displacements are assumed

$$\phi = \int p\ dt \qquad (6)$$

The aerodynamic moment coefficients and parameters used in the equations of motion previously given are presented in table I as functions of the three flight conditions used.

RESULTS AND DISCUSSION

Bank Command Loop

Selection of roll damper gain.- In figure 2 the effect of the roll damper gain K_4 on the roll response is shown for several values of K_4 at altitudes of 100,000, 150,000, and 210,000 feet. Bank angle and aileron-control deflections are shown plotted against time. A value of ϕ_c of $45°$ is used with bank command loop gain of $K_3 = 23$ and $K_5 = 2.5$. A yaw damper was used to provide damping in the lateral modes of oscillation.

An examination of figure 2 shows that the roll response times vary in the usual sense with dynamic pressure (table I), with the fastest response time of less than a second occurring at the maximum dynamic pressure (fig. 2(b)) and the slowest response time of about 2 seconds occurring at the minimum dynamic pressure (fig. 2(c)). The aileron-control motion is characterized by considerable limiting in figure 2 as it is throughout the entire investigation and is due principally to the rather large value of K_3 that was used.

The roll damper gain required for satisfactory roll response also changes with flight condition. In figure 2(b) a satisfactory roll response is obtained

with a roll damper gain of 2.0. However, a roll damper gain of 2.0 results in a much more oscillatory roll response at 100,000 feet (fig. 2(a)) than at 150,000 feet. Increasing the value of K_4 to 3.0 in figure 2(a) produces a better damped and more satisfactory roll response. At 210,000 feet (fig. 2(c)) an even larger value of K_4 is required since the dynamic pressure is smallest at this flight condition. A roll damper gain of 5.0 was considered satisfactory at the 210,000-foot flight condition. Roll response results were also obtained for values of ϕ_c of 30° and 15° by using roll damper gains found satisfactory for $\phi_c = 45°$, but are not presented. However, results did show satisfactory roll responses for the smaller values of ϕ_c although as might be expected the roll responses were better damped and somewhat slower.

Before a final selection of K_4 is made it is necessary to consider the complete motion of the bank command loop and the effect of yaw- and sideslip-rate dampers since the choice of dampers would probably require an adjustment of K_4.

Comparison of yaw- and sideslip-rate dampers.- Since damping augmentation in the lateral modes is required to provide satisfactory lateral stability of the vehicle during rolling maneuver in the flight region considered, the question of whether a yaw- or sideslip-rate damper is more desirable is examined. The effects of yaw- and sideslip-rate dampers on the vehicle lateral responses are shown in figures 3 and 4, respectively. The 150,000-foot flight condition was chosen for the comparison since it represented the flight condition with maximum dynamic pressure and corresponding faster vehicle responses. The variables ϕ, δ_a, δ_r, β, and r are plotted against time for damper gains K_5 of 0.5, 3.0, and 10.0. A step input of $\phi_c = 45°$ is used and a roll damper gain K_4 of 2.0 found satisfactory at this flight condition (fig. 2(b)) is also used. A roll damper gain of 2.5 is used for one curve in figure 4(b) as is explained subsequently.

Examination of figure 3 shows that rather large transient sideslip angles occur during the roll response at this flight condition. Even though the range of yaw damper gains has considerable effect on the damping of sideslip and yaw rate following the initial roll disturbance, the yaw damper itself has little effect on the magnitude of the initial sideslip disturbance. The minimum sideslip angle which occurs is 16.5° and represents a lateral acceleration of 1.30g at this flight condition. Since the range of yaw damper gains has little effect on the roll response, only one roll response is plotted for clarity.

Examination of figure 4, excluding the curves corresponding to $K_4 = 2.5$, shows that the sideslip-angle excursion following the initial roll disturbance decreases in magnitude as the sideslip damper gain increases. Notice also that the yaw rates are larger in magnitude following the roll disturbance for the larger sideslip damper gain. The larger yaw rates which are obtained through the $C_{n_{\delta_r}}$ term in the yaw equation with the larger sideslip damper gains are responsible for the smaller sideslip angle since the vehicle is tending to coordinate a turn. A sideslip damper gain of 3.0 appears to be the most

satisfactory at this flight condition since its use results in about the smallest β obtainable, and it has the advantage of a better damped β motion than is evident with the use of a gain of 10.0.

Unlike the yaw damper, the sideslip damper affects the roll response by tending to produce roll overshoot as the sideslip damper gain increases. The roll overshoot is the result of decreasing the opposing rolling moment due to β in the rolling-moment equation. Figure 4(b) also shows the case where K_4 is increased from 2.0 to 2.5 to reduce the roll overshoot present in the satisfactory case where $K_5 = 3.0$. Increasing K_4 from 2.0 to 2.5 has little effect on the vehicle motion except to reduce the roll overshoot. The general procedure of adjusting K_4 after the selection of a sideslip damper gain at each flight condition is followed. The amount of adjustment necessary depends primarily upon the amount the sideslip angle can be reduced which in turn depends upon the effectiveness of $C_{n_{\delta_r}}$ which varies with flight conditions. Since the utilization of a sideslip damper resulted in smaller sideslip angle than the use of a yaw damper as well as providing satisfactory overall system stability, it was decided that a sideslip damper was suitable and would be used in the evaluation of the complete control system.

Results of using a sideslip damper at the two other flight conditions are shown in figures 5 and 6. The same variables are plotted against time as in figures 3 and 4. A range of sideslip damper gains was used. Roll-rate damper gains found acceptable (as far as roll response is concerned) with the use of a yaw damper at each flight condition (fig. 2) are used together with an adjusted roll damper gain to reduce roll overshoot due to the sideslip damper. Examination of figure 5 (h = 100,000 feet) shows that the magnitude of sideslip angle is very small at this flight condition (compared with the 150,000-foot flight condition). The fact that the sideslip angle was reduced considerably by using the sideslip damper is evident by the considerable roll overshoot since the roll damper gain of 3.0 was originally adjusted for little or no overshoot with a yaw damper. The fact that β can be reduced to such a small value as indicated previously is the result of a more effective $C_{n_{\delta_r}}$ term in the yaw equation at this flight condition as shown in table I. A sideslip damper gain of 10.0 appears to be the most satisfactory at this flight condition together with a roll damper gain of 5.0 to reduce the roll overshoot.

Inspection of figure 6 shows that at 210,000 feet the sideslip damper does not succeed in reducing the magnitude of sideslip as well as at the 100,000-foot flight condition, but the magnitude produced is comparable to results from the 150,000-foot flight condition (fig. 4). On this basis, it is interesting to note that the values of $C_{n_{\delta_r}}$ at the 150,000- and 210,000-foot flight conditions are comparable whereas at the 100,000-foot flight condition the value is approximately twice that of the 150,000- and 210,000-foot flight conditions. It is also interesting to note that the roll overshoot evident in figure 6 is not as pronounced as it was in figure 5. A sideslip damper gain of 3.0 appears more desirable at this flight condition since its use yields about the smallest value of β possible and results in a fairly damped sideslip and yaw motion.

Finally, the selection of $K_5 = 3.0$ at the 150,000- and 210,000-foot flight conditions, and $K_5 = 10.0$ at the 100,000-foot flight condition, appears to be the most satisfactory. However, the choice of $K_5 = 3.0$ over the complete flight region would also provide satisfactory damping and have the advantage of simplifying the selection of K_5 during reentry. The use of $K_5 = 3.0$ over the complete flight region would result in larger sideslip angles at the 100,000-foot flight condition than would be necessary (fig. 5), but its use would still provide smaller sideslip angles at the 100,000-foot flight condition than at the 150,000- and 210,000-foot flight conditions.

Complete Control System

For the analyses of the complete control system all bank command loop gains are held fixed at values found suitable at each flight condition. The gain K_2 is also held constant at a value of 50 during the analysis at each flight condition. This value of K_2 was found to provide adequate damping of the heading-angle response following a heading-angle-command step input. For the study of the complete control system a range of step input values of $\psi_{w,c}$ from 0.25° to 2.0° is used and the heading-angle-error gain K_1 is varied in order to provide satisfactory heading-angle response as well as satisfactory overall system response at each flight condition. Figures 7, 8, and 9 show the effect of step inputs of $\psi_{w,c}$ on the vehicle lateral responses at the 100,000-, 150,000-, and 210,000-foot flight conditions, respectively. Time histories of the system variables ψ_w, ϕ, ϕ_c, β, and r are shown.

Figure 7(a) with $\psi_{w,c} = 0.25^\circ$ shows a range of heading-angle responses from overdamped $(K_1 = 90)$ to underdamped $\left(K_1 = 150, \; K_1 \approx 160\right)$. The variable ϕ_c never reaches the limit of 45° and ϕ itself never exceeds 18°. Thus, the maximum heading-rate capability for $\phi = 45^\circ$ is not utilized for the small $\psi_{w,c}$ value. Both β (only one curve is used to represent the β motion in the interest of clarity) and r do not experience the magnitude present in figure 5 (bank command loop) as the result of the smaller amplitude of ϕ in figure 7(a) compared with the larger ϕ of 45° in figure 5. Figure 7(b) shows the results of increasing $\psi_{w,c}$ from 0.25° to 0.5°. A comparison of the two cases of $K_1 = 150$ in figures 7(a) and 7(b) shows that increasing $\psi_{w,c}$ from 0.25° to 0.5° results in creating instability and divergent motion of the control system. However, when K_1 is reduced to a value of 115 the control-system response becomes fairly well behaved and may be considered satisfactory. Notice also that larger magnitudes of ϕ_c, ϕ, β, and r are present for K_1 of 115 in figure 7(b) than in figure 7(a). This result is expected since $\psi_{w,c}$ is larger in figure 7(b).

Figure 7(c) shows the result of increasing $\psi_{w,c}$ from 0.5° to values of 1.0° and 2.0°. When the two cases of $K_1 = 115$ are compared in figures 7(b)

and 7(c) for $\psi_{w,c}$ values of 0.5° and 1.0°, it is observed that increasing $\psi_{w,c}$ again tends to destabilize the vehicle response with resulting increased oscillations. However, when K_1 is reduced to a value of 90 for $\psi_{w,c}$ of 1.0°, the vehicle motion becomes more satisfactory. When $\psi_{w,c}$ is increased from 1.0° to 2.0° for $K_1 = 90$, it is observed that the increase tends to stabilize the system. Values of $\psi_{w,c}$ up to 5.0 were used at this flight condition (though not presented), and results showed that a value of K_1 of 90 was satisfactory for $\psi_{w,c}$ values of 2.0° to 5.0°. The result that K_1 must decrease with increasing $\psi_{w,c}$ input to produce satisfactory vehicle responses is not an unexpected result for a control system being saturated (ϕ_c limiting) with a $\psi_{w,c}$ input. In reference 6 the author shows the nonlinear relationship that must hold for a lower order system between an error gain and input for a time-optimum response.

From results presented (fig. 7) it is evident that at this flight condition K_1 cannot exceed 90 for system stability if K_1 is to be held at a constant value for the complete range of $\psi_{w,c}$ values. Using a constant K_1 of 90 (as opposed to perhaps generating K_1 as a function of $\psi_{w,c}$) for a range of $\psi_{w,c}$ values appears to be more satisfactory since it is the simplest method. Also, its use does not sufficiently penalize the vehicle response except to produce slower heading-angle responses for the smaller values of $\psi_{w,c}$ (figs. 7(a) and 7(b)) which may be tolerated in the interest of simplicity in selecting K_1.

Figure 8 shows the effect of $\psi_{w,c}$ on the vehicle lateral responses at 150,000 feet. A range of values for K_1 is used. Inspection of figure 8(a) ($\psi_{w,c} = 0.25^\circ$) shows that much larger values of K_1 are required to cause a ψ_w overshoot at 150,000 feet than at 100,000 feet (fig. 7(a)). A control-system gain K_1 of 300, which causes a ψ_w overshoot for $\psi_{w,c} = 0.25^\circ$, does not result in an overshoot for $\psi_{w,c} = 0.50^\circ$. Thus, it appears that the problem of decreasing K_1 as $\psi_{w,c}$ increases is not as critical at 150,000 feet as it was at 100,000 feet. The reason is attributed to the fact that the quantity $\dfrac{0.906L}{mV}$ (table I) is much smaller at 150,000 feet than it is at 100,000 feet. As a result smaller heading-angle rates exist for a given value of ϕ. The slower heading-rate responses due to the smaller value of $\dfrac{L}{mV}$ can be quickened by increasing K_1 to generate larger values of ϕ for the smaller $\psi_{w,c}$ values. When $\psi_{w,c}$ is increased sufficiently to a value of 2.0° (fig. 8(d)) ϕ_c is characterized by considerable limiting due to the relatively large $\psi_{w,c}$ input. As a result, the first portion of the vehicle response

11

(ϕ_c limited) is identical to the inner loop case for $\phi_c = 45°$, $K_4 = 2.5$, and $K_5 = 3.0$. (See fig. 4(b).)

The extensive limiting of ϕ_c (fig. 8(d)), as opposed to short-time limiting of ϕ_c, is beneficial as it allows the transient motion following the initial control-system disturbance to damp out before the system is disturbed again by ϕ_c coming off the limits. As a result smaller negative magnitudes of sideslip angle are present for the largest values of $\psi_{w,c}$ (fig. 8(d)) than for the smaller values of $\psi_{w,c}$ (figs. 8(a), 8(b), and 8(c)) where ϕ_c limiting occurs.

Examination of figure 8 shows that a value of K_1 of 200 would provide a satisfactory rapid heading-angle response. However, in the interest of keeping K_1 constant over the range of flight conditions, it appears that a K_1 of 90 would also appear satisfactory at this flight condition, and that the faster heading-angle responses with $K_1 = 200$ are not as advantageous as the simplicity of a constant K_1 over the complete flight region. Keeping K_1 small also has the advantage that smaller β magnitudes are generated. (See, for example, figs. 8(a) and 8(b) for cases of $K_1 = 200$ and $K_1 = 90$.)

Finally, figure 9 shows the effect of using a K_1 of 90 at 210,000 feet. Because the value of $\frac{0.906L}{mV}$ is much smaller at this flight condition than at the previous two flight conditions, the heading-angle response times are much longer with the heading-angle response time at $\psi_{w,c} = 2.0°$ taking about 50 seconds for ψ_w to reach $2.0°$. It is believed that $K_1 = 90$ provides satisfactory heading response times for the range of $\psi_{w,c}$ values utilized as evidenced by considerable bank-angle limiting at $45°$ (maximum $\dot{\psi}_w$) for the two larger $\psi_{w,c}$ values.

<div align="center">CONCLUDING REMARKS</div>

An investigation has been made to determine the capability of a proportional-type lateral control system of providing aerodynamic heading-angle control of a vehicle having a maximum lift-drag ratio of 2 during reentry into the earth's atmosphere. Results indicate that the control system is capable of providing satisfactory heading-angle control over the flight region considered. A sideslip damper was found more suitable than a yaw damper since its use resulted in smaller sideslip angles during the rolling maneuver. The sideslip damper gain was required to vary over the flight region if minimum sideslip at each flight condition was to be obtained. However, results obtained tend to indicate that the sideslip damper could be held constant over the complete flight region at a value of 3.0 and still provide satisfactory damping in side-slip. The roll damper gain was required to vary over the flight region as the result of the large range of dynamic pressures.

The heading-error gain was found to be dependent upon the command heading angle particularly at the 100,000-foot flight condition if as rapid a heading-angle response as possible was to be obtained. However, results also show that the heading-error gain could be held at a constant value of 90 over the complete flight region and still provide satisfactory vehicle responses though the heading-angle response time at the smaller values of command heading angle tended to be somewhat slower than if larger heading-error gains were used. The heading-error gain of 90 represents the largest gain value that could be tolerated over the complete flight region if control-system stability is to be maintained.

Finally, if the sideslip damper gain and the heading-error gain are held constant over the complete flight region (as results indicate they could be), the only gain of the control system that need be varied during reentry is the roll damper gain. This is evidently desirable as it greatly simplifies the mechanization of gain control during reentry.

Langley Research Center,
    National Aeronautics and Space Administration,
        Langley Station, Hampton, Va., February 28, 1964.

DERIVATION OF HEADING-RATE EQUATION

From reference 5, the rate of change of the vehicle wind heading angle is

$$\dot{\psi}_W = \frac{1}{\cos \theta_W}(R_W \cos \phi_W + Q_W \sin \phi_W)$$

where θ_W and ϕ_W are Euler angles as measured in wind axes. The terms R_W and Q_W are related to the force terms in the wind-axis system as follows (from ref. 5):

$$R_W = \frac{F_{W,Y}}{mV}$$

$$Q_W = -\frac{F_{W,Z}}{mV}$$

where $F_{W,Y}$ and $F_{W,Z}$ are aerodynamic forces along Y_W and Z_W, respectively. Substituting the equations of $F_{W,Y}$ and $F_{W,Z}$ from reference 5 into the equations of R_W and Q_W yields

$$R_W = \frac{1}{mV}\left(-F_{S,X} \sin \beta + F_{S,Y} \cos \beta\right)$$

$$Q_W = -\frac{F_{S,Z}}{mV}$$

where $F_{S,X}$, $F_{S,Y}$, and $F_{S,Z}$ are aerodynamic forces acting along X_S, Y_S, and Z_S, respectively. The aerodynamic forces along the stability axes are

$$F_{S,X} = -D \cos \beta$$

$$F_{S,Y} = -D \sin \beta + Y$$

$$F_{S,Z} = -L$$

where L and D are, respectively, lift and drag. The term Y is side force defined by the equation

$$Y = qSC_{Y_\beta}\beta$$

Substituting the equations of $F_{S,X}$, $F_{S,Y}$, and $F_{S,Z}$ into the equations of R_W and Q_W yields

$$R_W = \frac{Y \cos \beta}{mV}$$

$$Q_W = \frac{L}{mV}$$

Finally, substituting R_W and Q_W into the equation of $\dot{\psi}_W$ yields

$$\dot{\psi}_W = \frac{1}{mV \cos \theta_W}(Y \cos \beta \cos \phi_W + L \sin \phi_W)$$

Since $\theta_W = \gamma = 0$

$$\dot{\psi}_W = \frac{1}{mV}(Y \cos \beta \cos \phi_W + L \sin \phi_W)$$

For a coordinated turn maneuver ($\beta = Y = 0$)

$$\dot{\psi}_W = \frac{L \sin \phi_W}{mV}$$

In order to determine ϕ_W in terms of body bank angle ϕ, the equation of $\tan \phi_W$ (from ref. 5) is used with the assumption that $\beta = 0$ and $\theta = \alpha = 25^\circ$. These assumptions yield the equation

$$\tan \phi_W = \frac{0.906 \sin \phi}{0.179 + 0.821 \cos \phi}$$

A good approximation for $\sin \phi_W$ was found to be

$$\sin \phi_W = 0.906 \sin \phi$$

The substitution of $\sin \phi_W = 0.906 \sin \phi$ into the equation of $\dot{\psi}_W$ gives

$$\dot{\psi}_W = \frac{0.906L}{mV} \sin \phi$$

which may be written in the form

$$\psi_w = \frac{0.906L}{mV} \int_0^t \sin \phi \, dt$$

REFERENCES

1. Bryson, Arthur E., Mikami, Kinya, and Battle, C. Tucker: Optimum Lateral Turns for a Re-Entry Glider. Paper No. 62-6, Inst. Aerospace Sci., Jan. 1962.

2. Slye, Robert E.: An Analytical Method for Studying the Lateral Motion of Atmosphere Entry Vehicles. NASA TN D-325, 1960.

3. Young, John W.: A Method for Longitudinal and Lateral Range Control for a High-Drag Low-Lift Vehicle Entering the Atmosphere of a Rotating Earth. NASA TN D-954, 1961.

4. Sparrow, Gene W.: A Study of the Effects of Bank Angle, Banking Duration, and Trajectory Position of Initial Banking on the Lateral and Longitudinal Ranges of a Hypersonic Global Reentry Vehicle. NASA TN D-1617, 1963.

5. Howe, R. M.: Coordinate Systems for Solving the Three-Dimensional Flight Equations. WADC Tech. Note 55-747, U.S. Air Force, June 1956, pp. 8 to 13. (Available from ASTIA as AD 111582.)

6. Schmidt, Stanley Francis: The Analysis and Design of Continuous and Sampled-Data Feedback Control Systems With a Saturation Type Nonlinearity. NASA TN D-20, 1959.

TABLE I.- AERODYNAMIC MOMENT COEFFICIENTS AND PARAMETERS

$$\left[\alpha = 25^\circ; \; \gamma = 0^\circ\right]$$

	h = 100,000 ft	h = 150,000 ft	h = 210,000 ft
Mach number	3.03	12.43	14.50
Velocity, V, ft/sec	3,040	13,633	14,854
Dynamic pressure, q, lb/sq ft	153	327	47.0
Lift coefficient, C_L	0.422	0.369	0.369
$0.906L/mV$	0.0248	0.0103	0.00136
C_{l_p}, per radian	-0.305	-0.305	-0.305
C_{l_β}, per radian	-0.0321	-0.0321	-0.0321
$C_{l_{\delta_a}}$, per radian	0.149	0.174	0.174
C_{n_r}, per radian	-0.31	-0.27	-0.27
C_{n_β}, per radian	0.033	0.033	0.033
$C_{n_{\delta_r}}$, per radian	-0.0321	-0.0160	-0.0143
$C_{n_{\delta_a}}$, per radian	0.00106	-0.0031	-0.0031
C_{Y_β}, per radian	-0.361	-0.344	-0.344

18
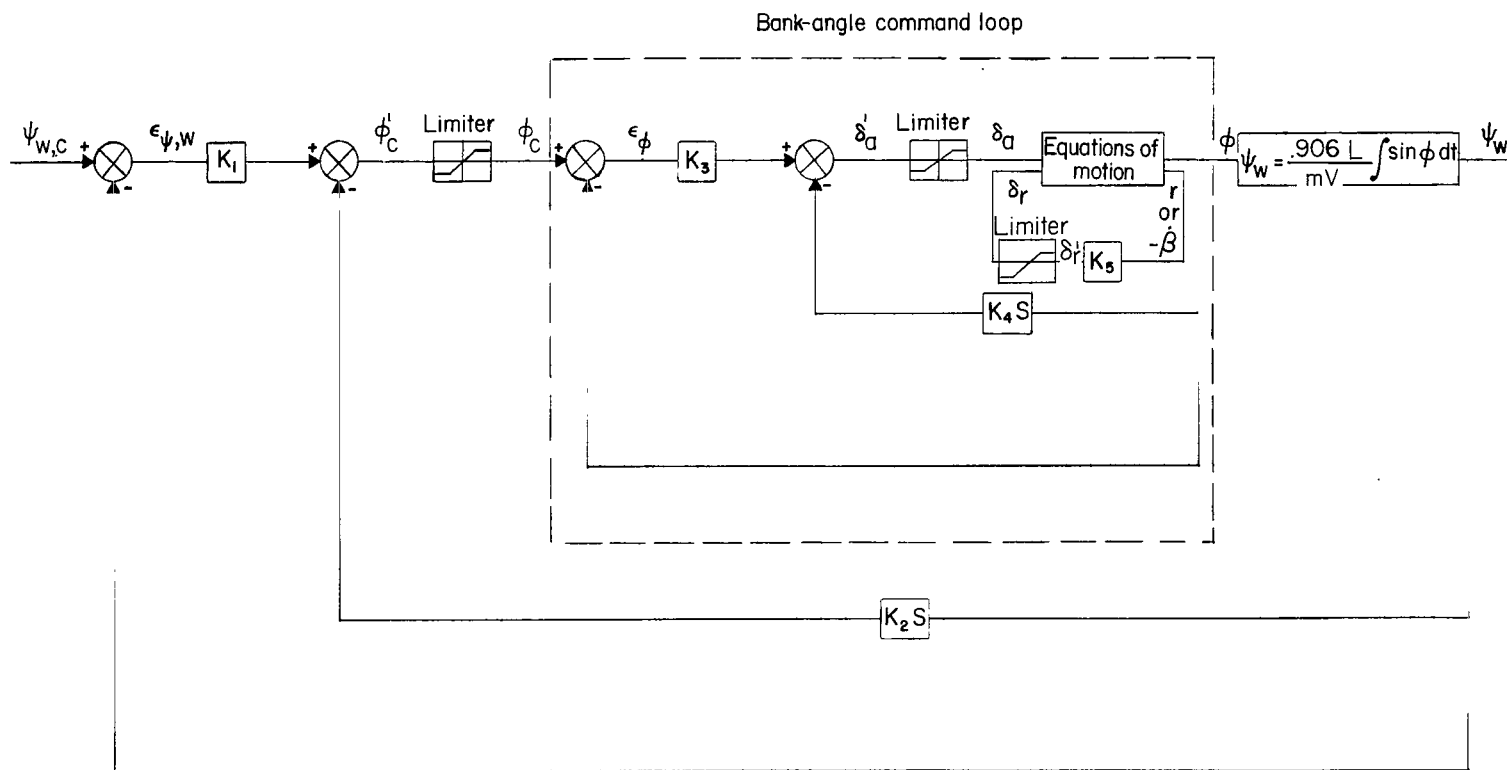
Figure 1.- Block diagram of heading-angle control system.
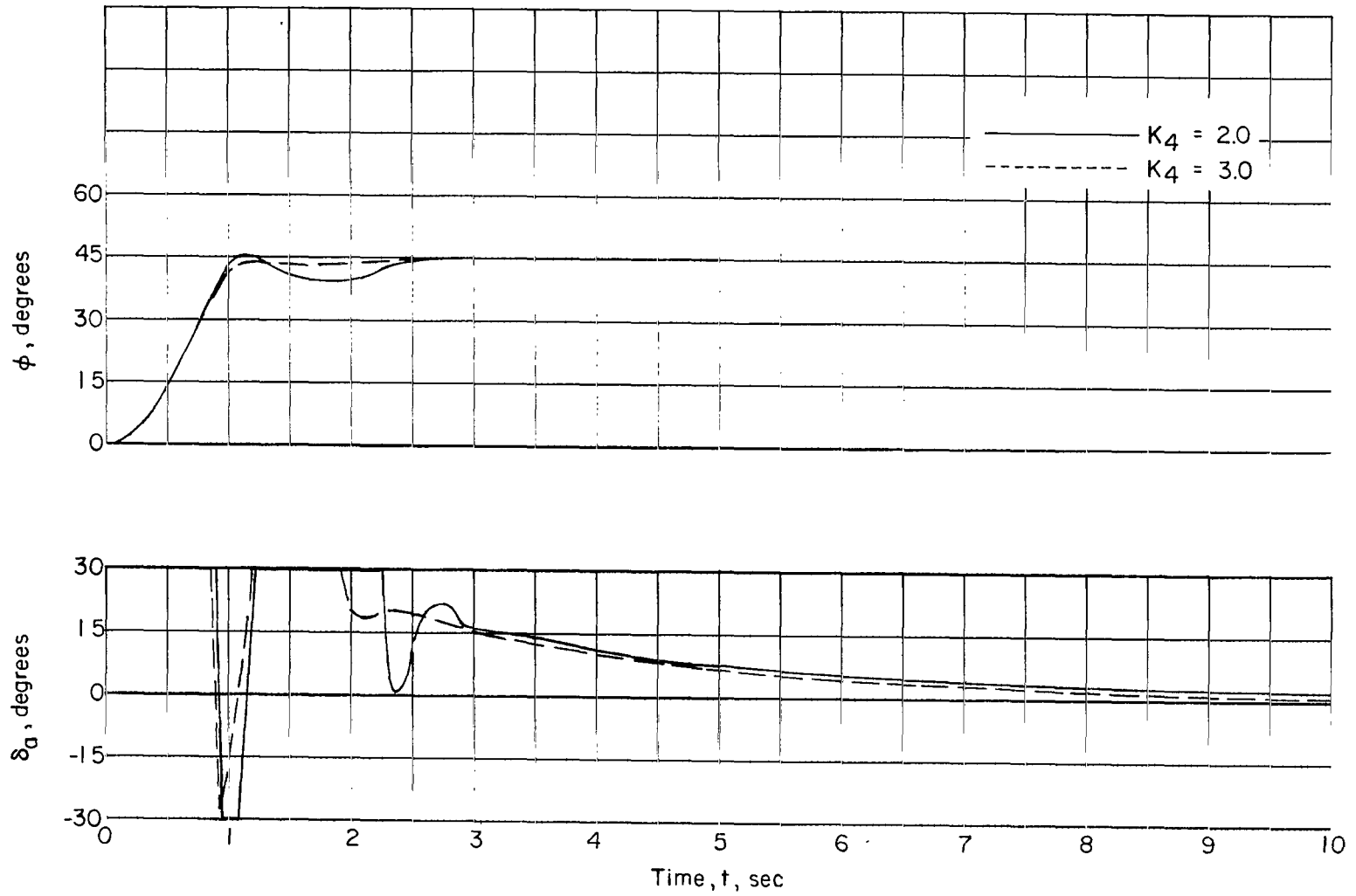
(a) h = 100,000 feet.

Figure 2.- Effect of roll damper gain on roll response. Yaw damper; $\phi_c = 45°$; $K_3 = 23.0$; $K_5 = 2.50$.
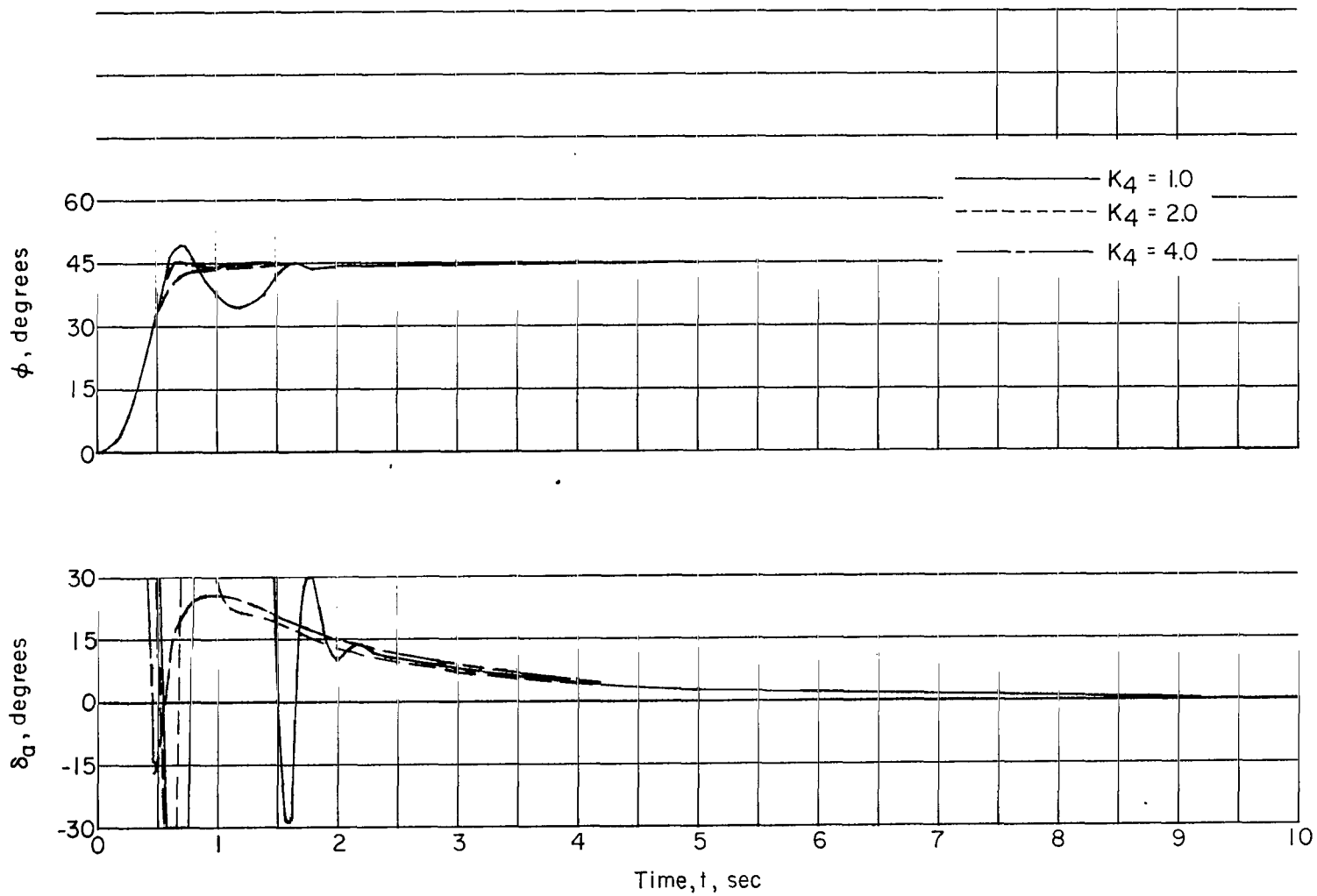
(b) h = 150,000 feet.

Figure 2.- Continued.
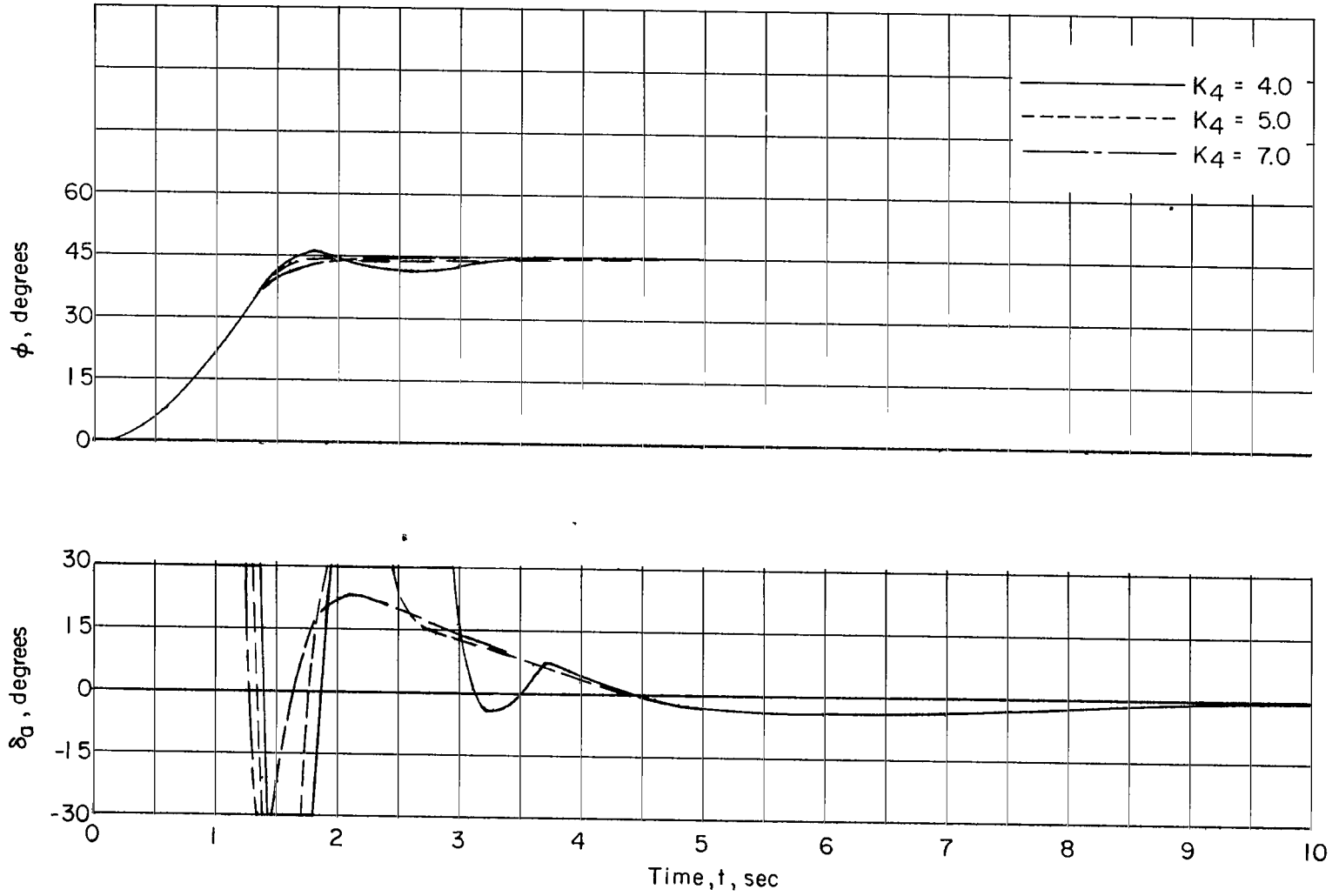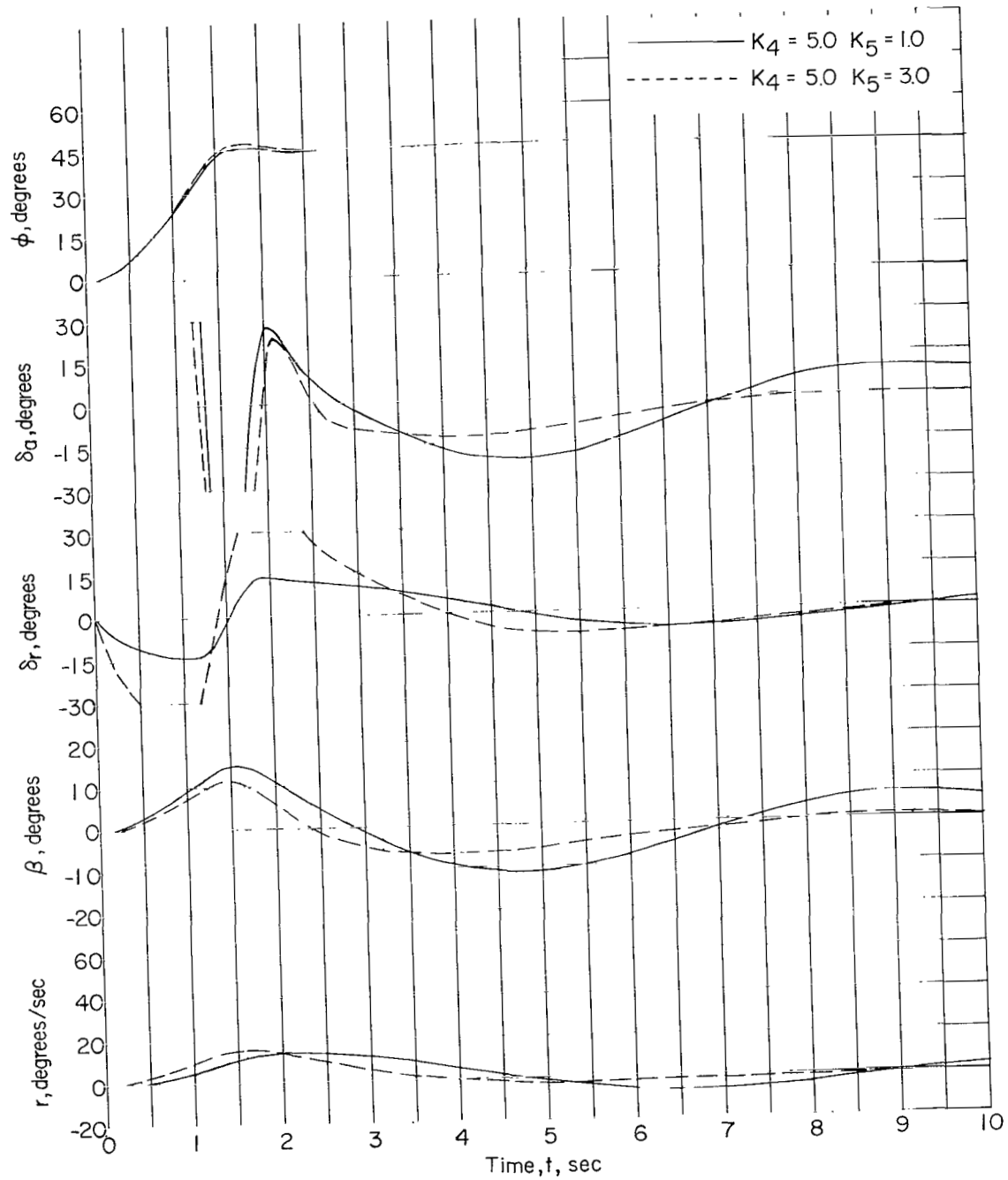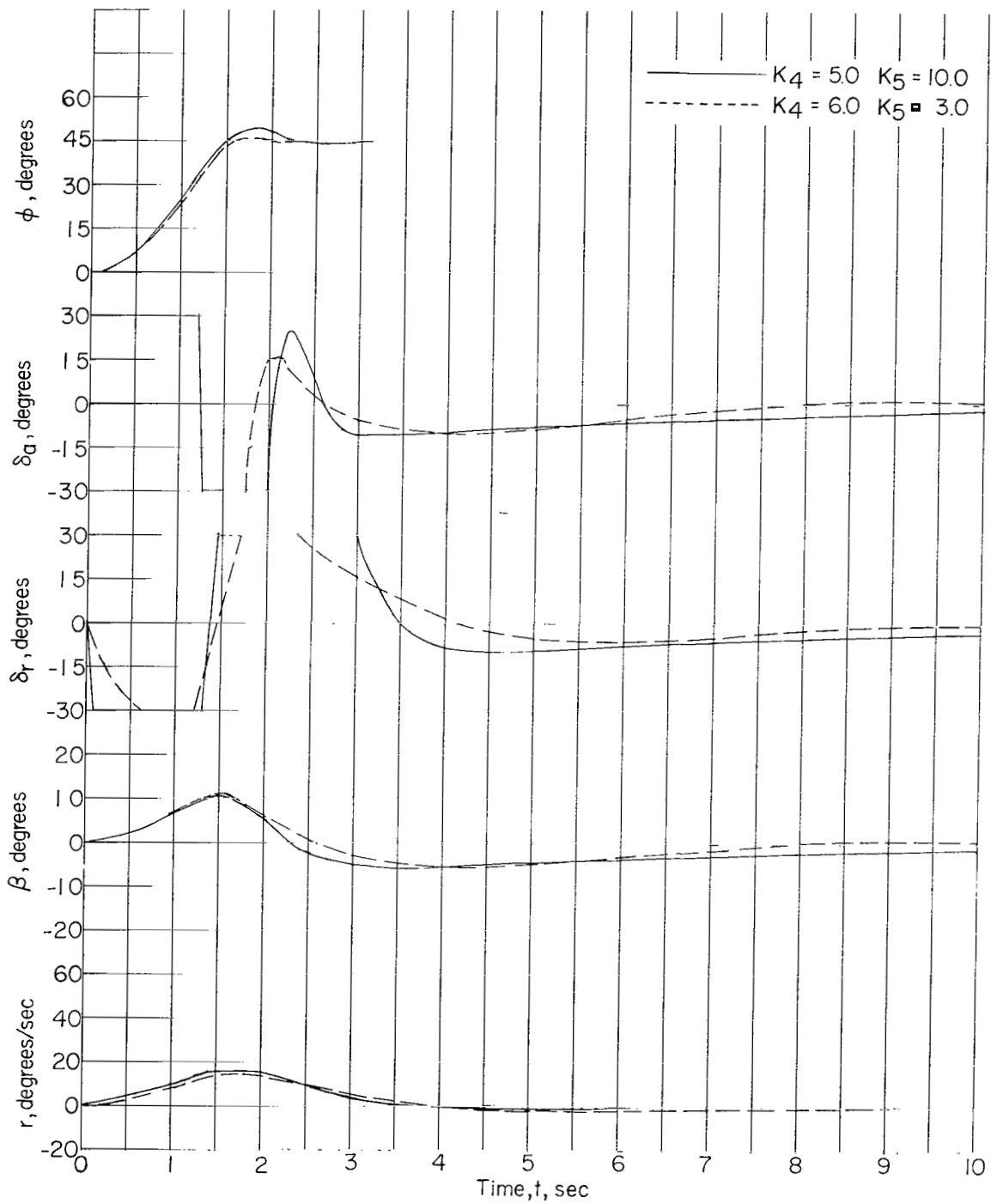
(c) h = 210,000 feet.

Figure 2.- Concluded.
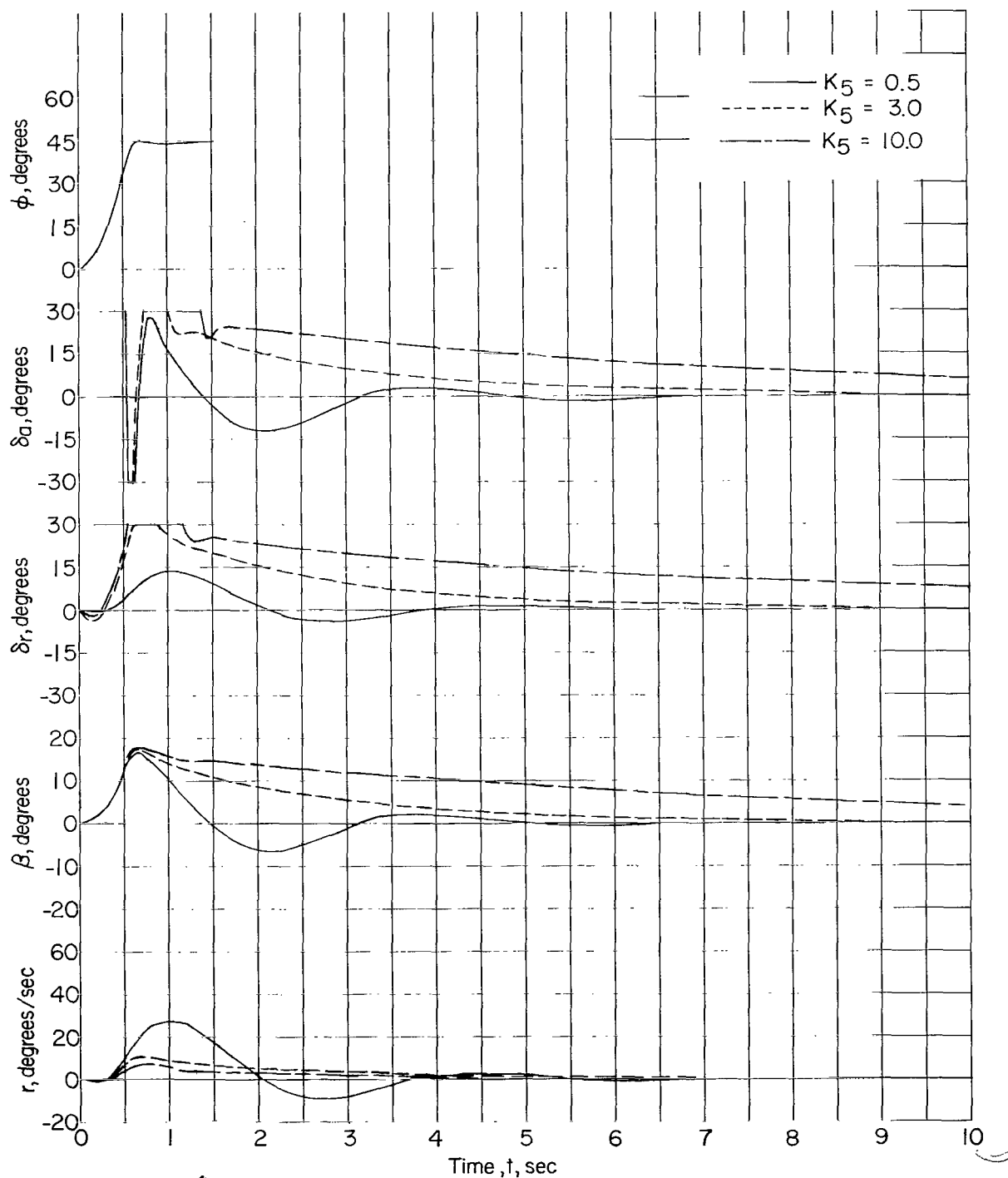
Figure 3.- Effect of yaw damper on vehicle lateral responses at 150,000 feet.
$\phi_c = 45°$; $K_3 = 23.0$; $K_4 = 2.0$.
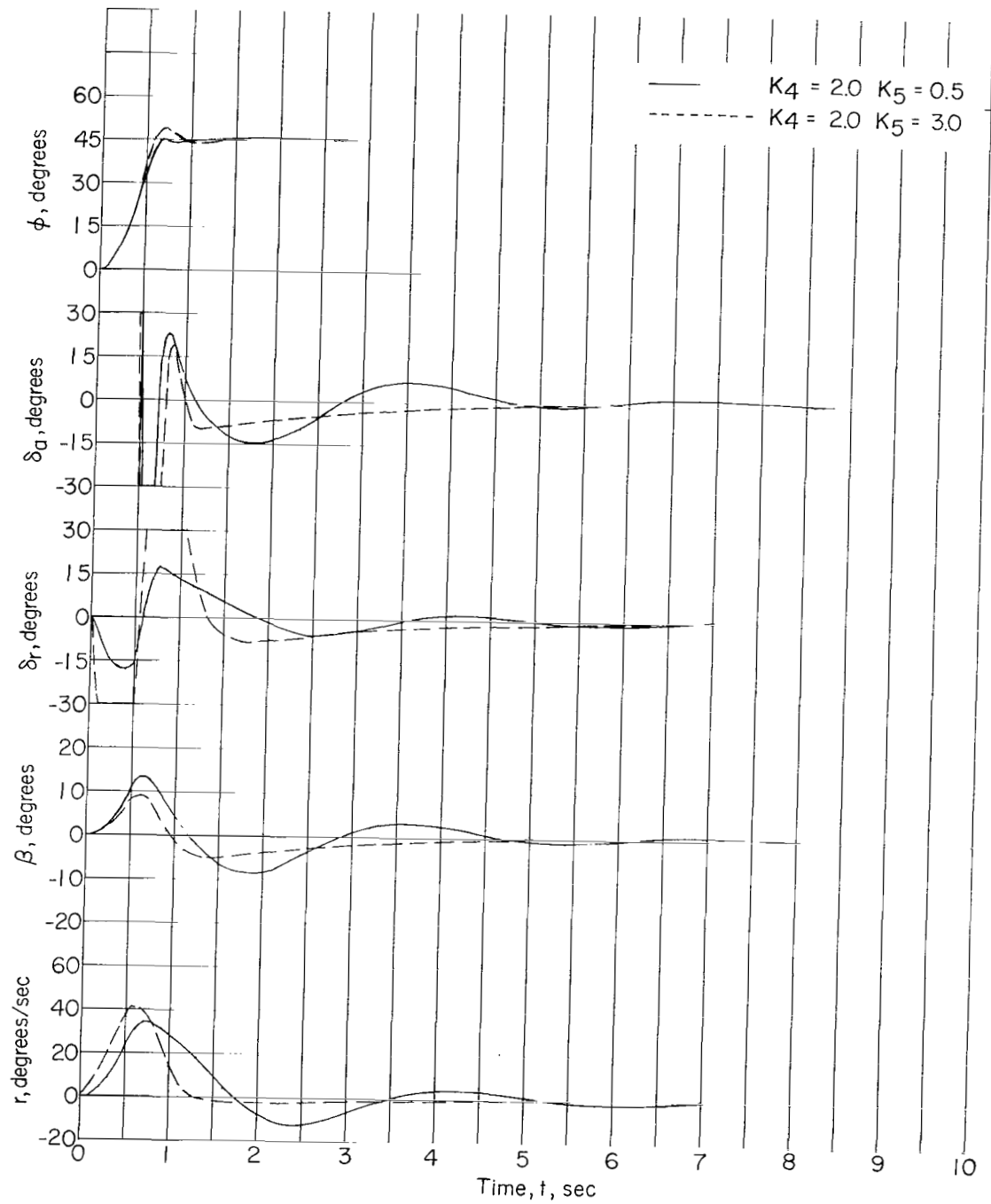
(a)

Figure 4.- Effect of sideslip damper on vehicle lateral responses at 150,000 feet. $\phi_c = 45°$; $K_3 = 23.0$.
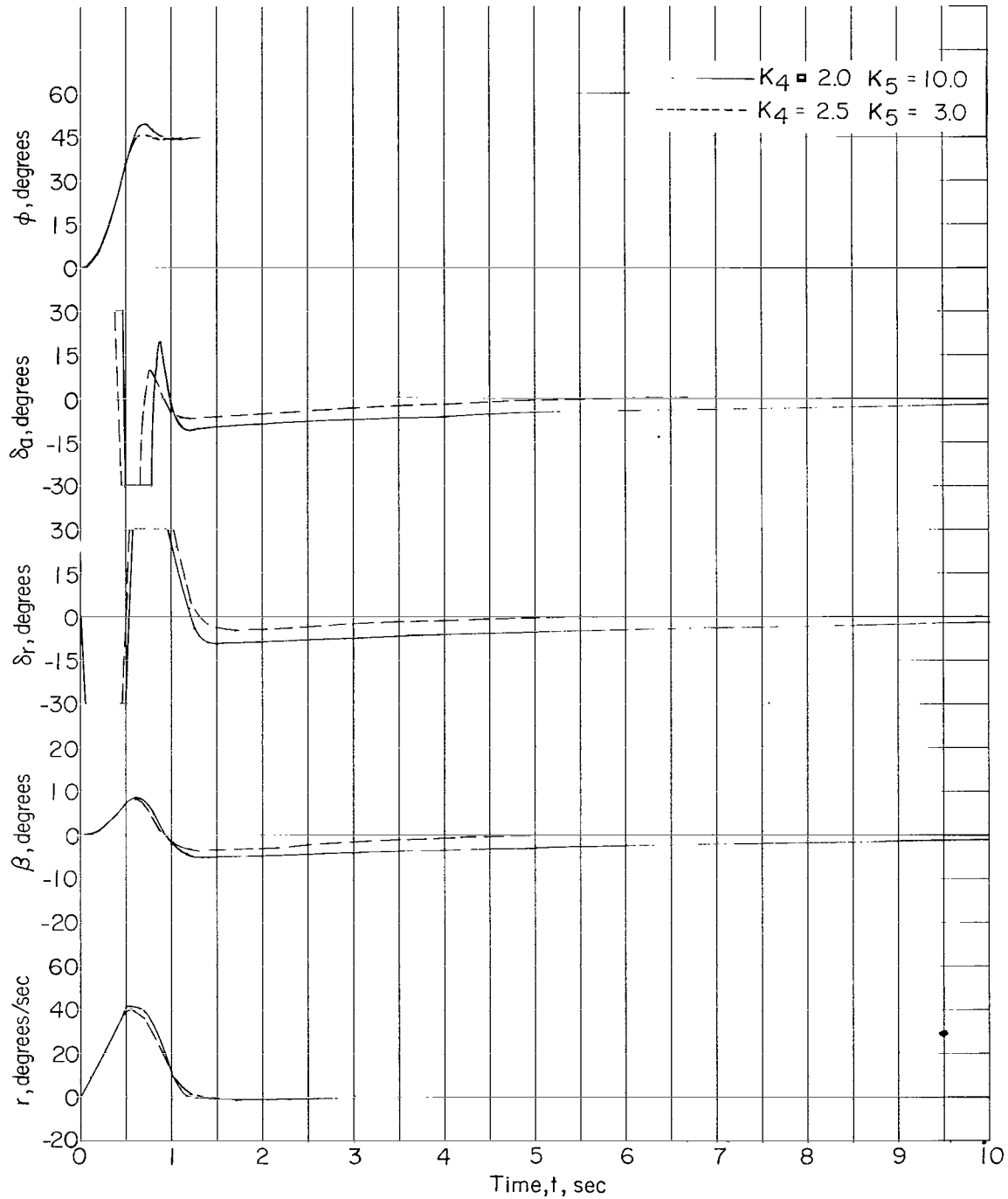
(b)

Figure 4.- Concluded.
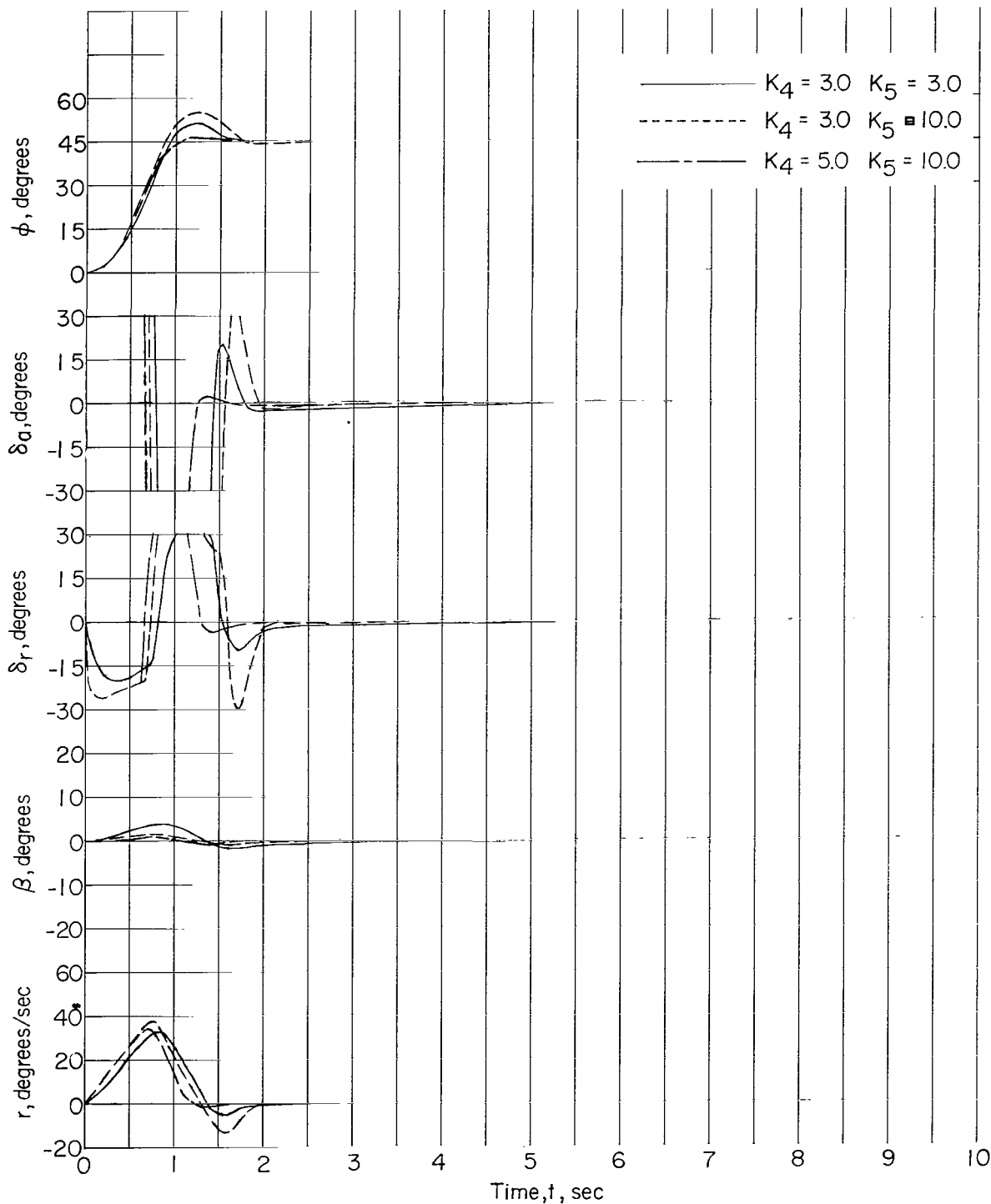
Figure 5.- Effect of sideslip damper on vehicle lateral responses at 100,000 feet.
$\phi_c = 45°$; $K_3 = 23.0$.

Figure 6.- Effect of sideslip damper on vehicle lateral responses at 210,000 feet.
$\phi_c = 45°$; $K_3 = 23.0$.

(b)

Figure 6.- Concluded.
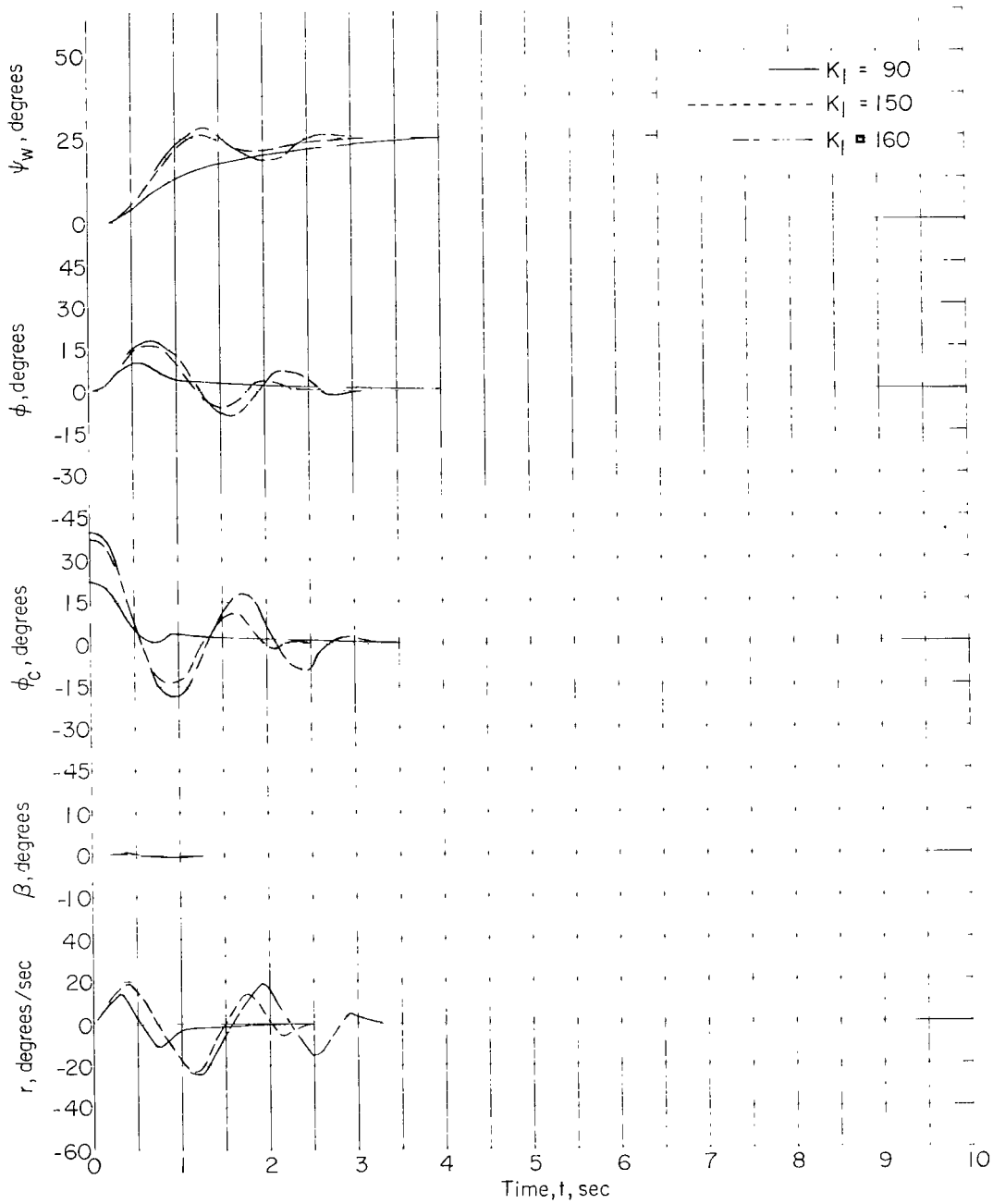
(a) $\psi_{w,c} = 0.25^\circ$.

Figure 7.- Effects of command heading angle and heading-error gain on vehicle lateral responses at 100,000 feet with sideslip damper. $K_2 = 50.0$; $K_3 = 23.0$; $K_4 = 5.00$; $K_5 = 10.0$.
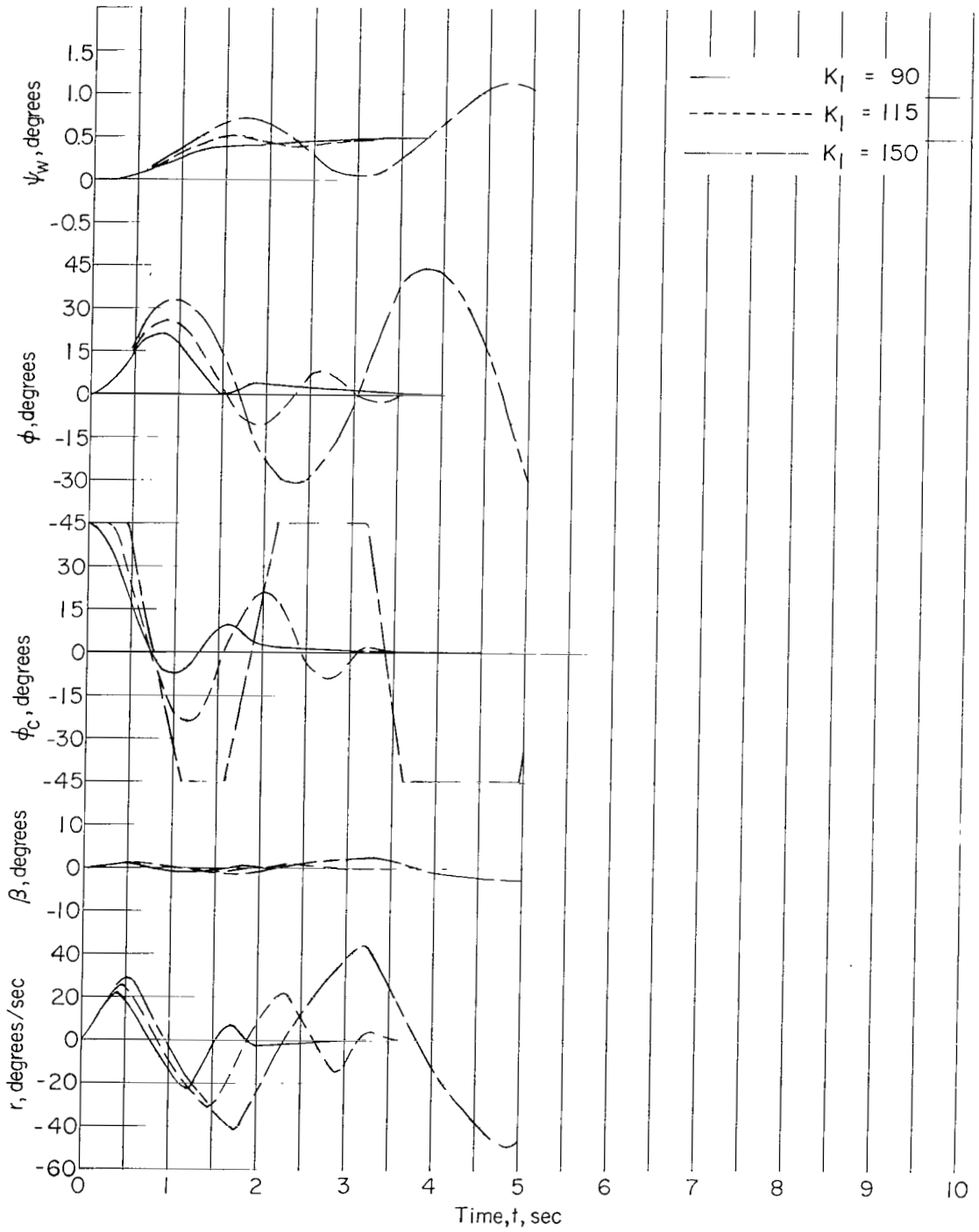
(b) $\psi_{w,c} = 0.50°$.

Figure 7.- Continued.
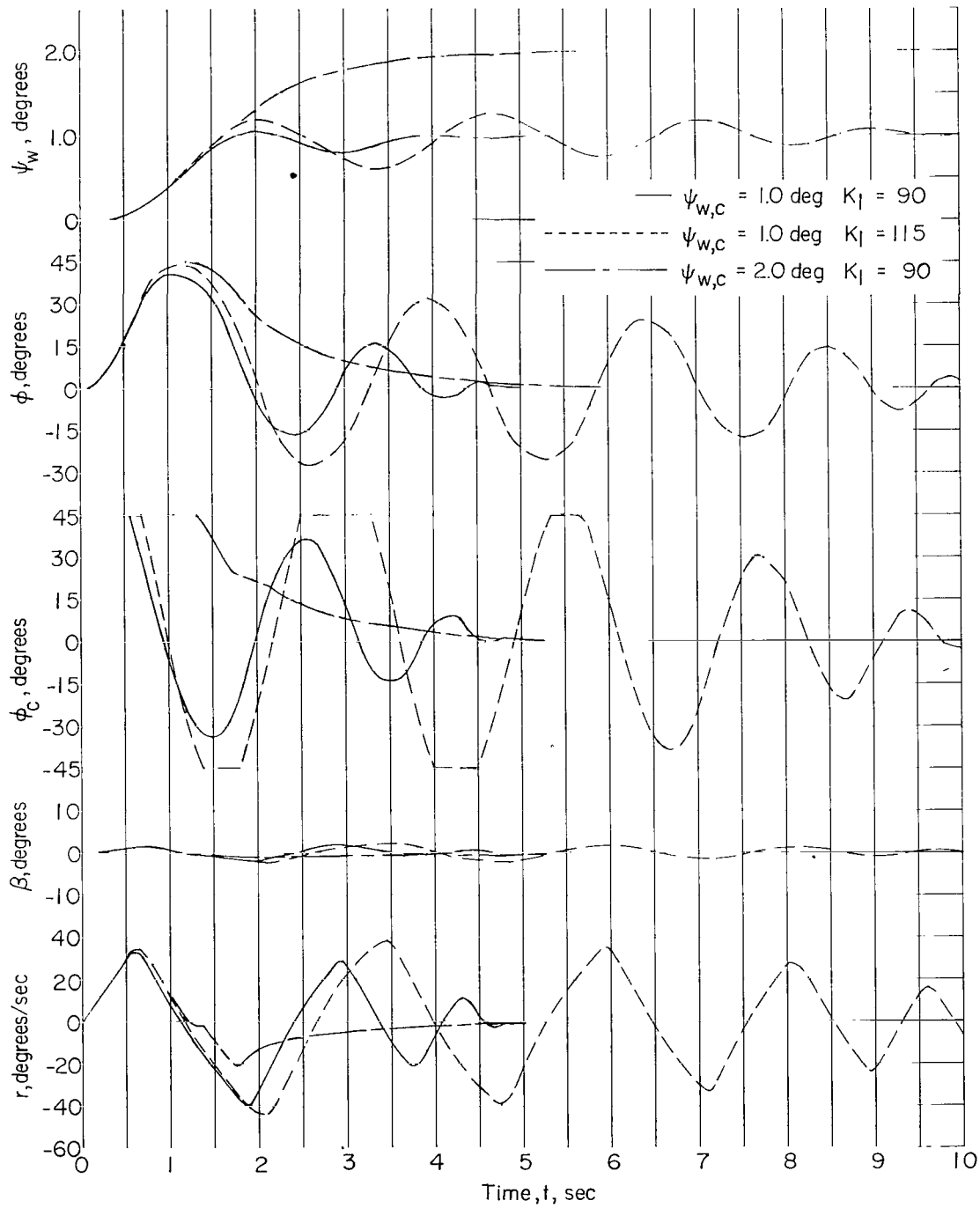
(c) $\psi_{w,c} = 1.0^{\circ}$; 2.0°.

Figure 7.- Concluded.
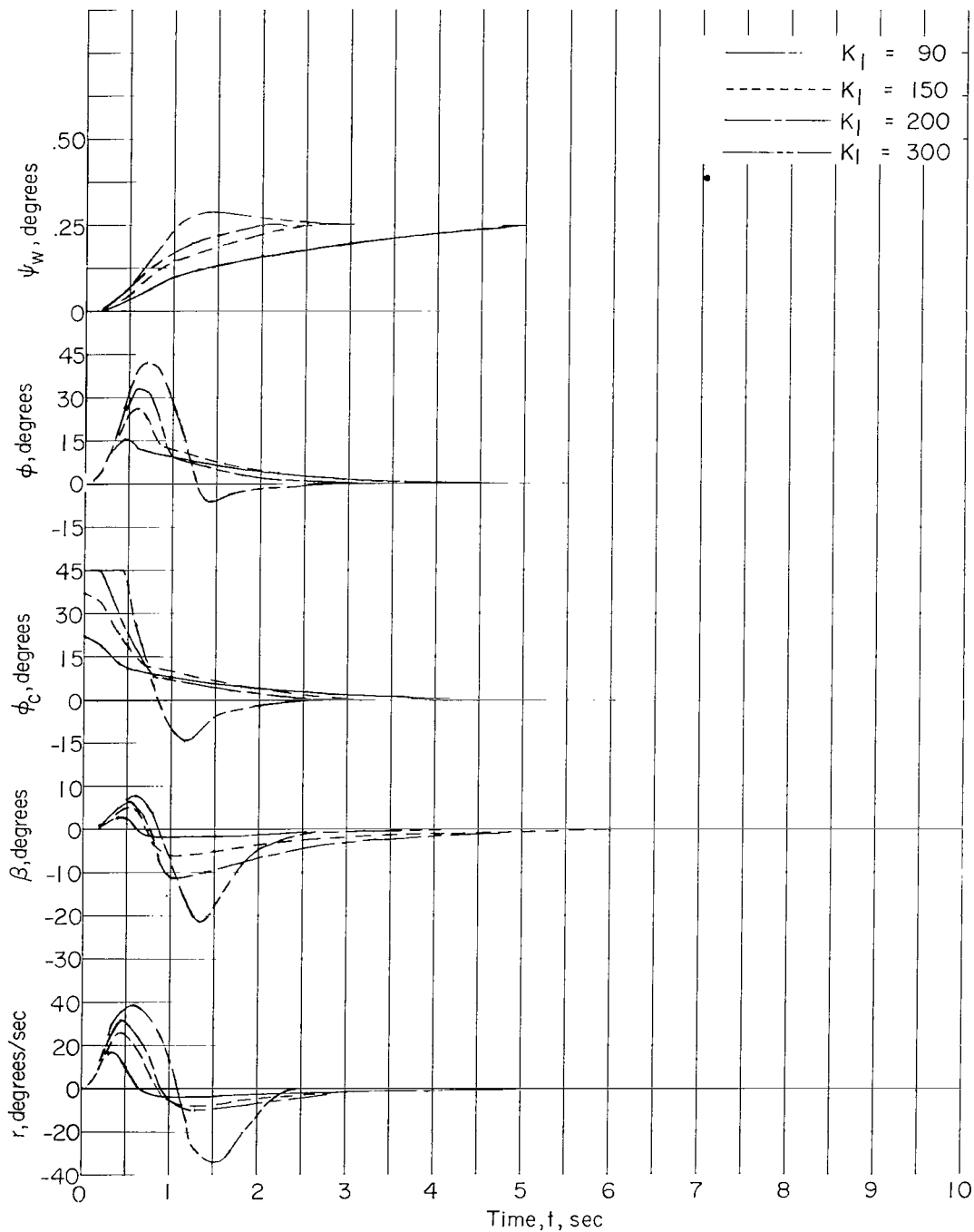
(a) $\psi_{w,c} = 0.25°$.

Figure 8.- Effects of command heading angle and heading-error gain on vehicle lateral responses at 150,000 feet with sideslip damper. $K_2 = 50.0$; $K_3 = 23.0$; $K_4 = 2.50$; $K_5 = 3.0$.
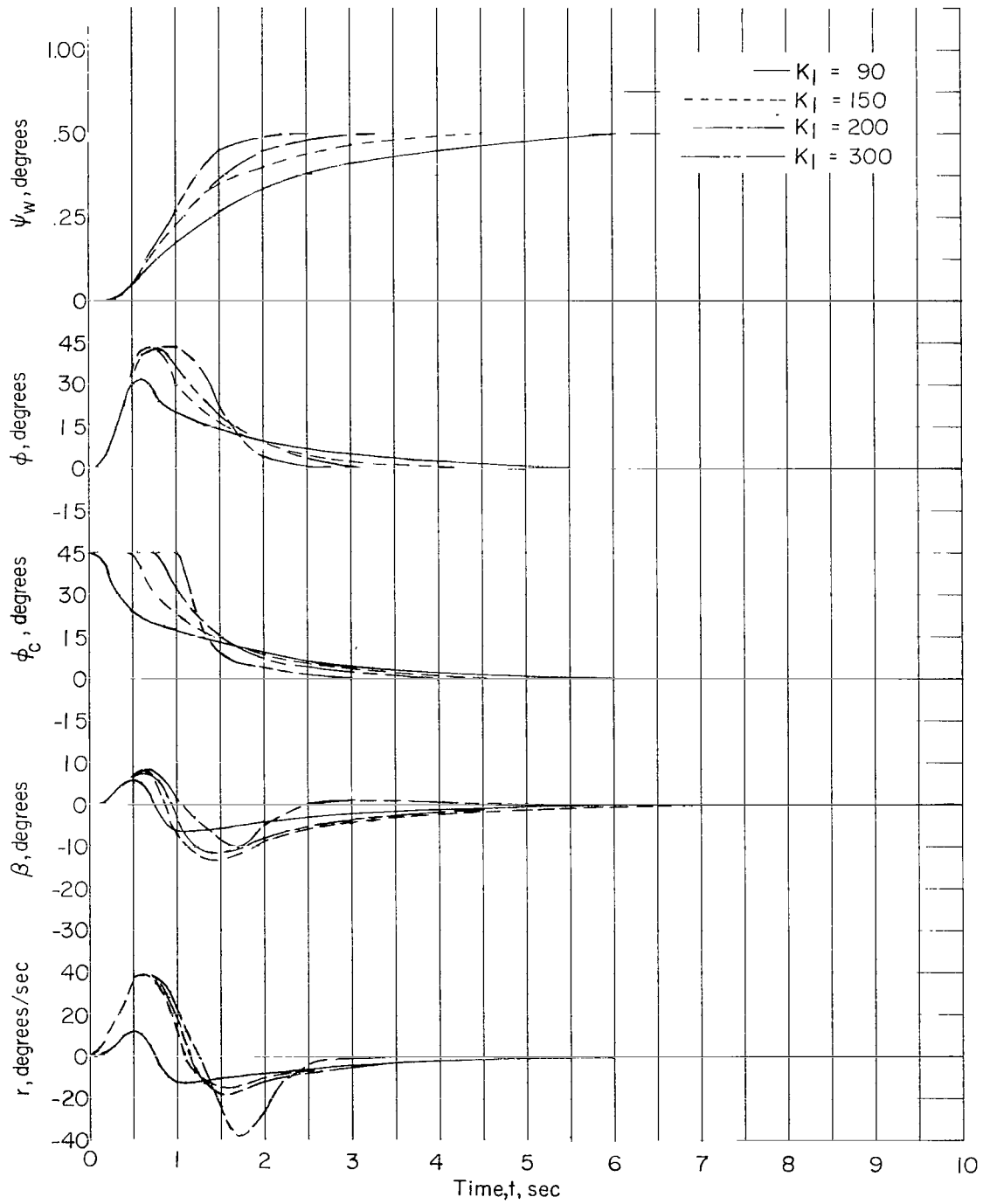
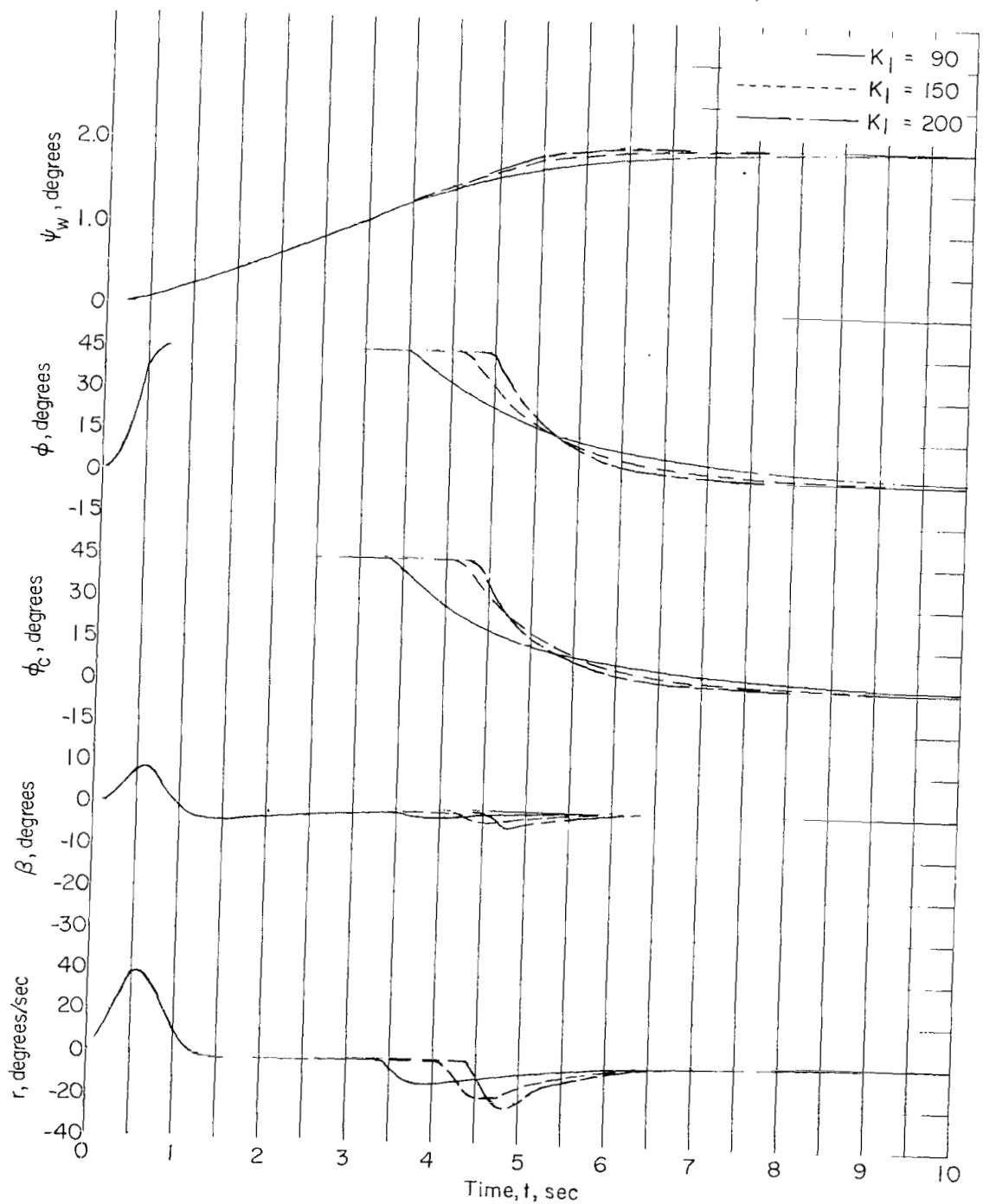(b) $\psi_{w,c} = 0.50°$.

Figure 8.- Continued.
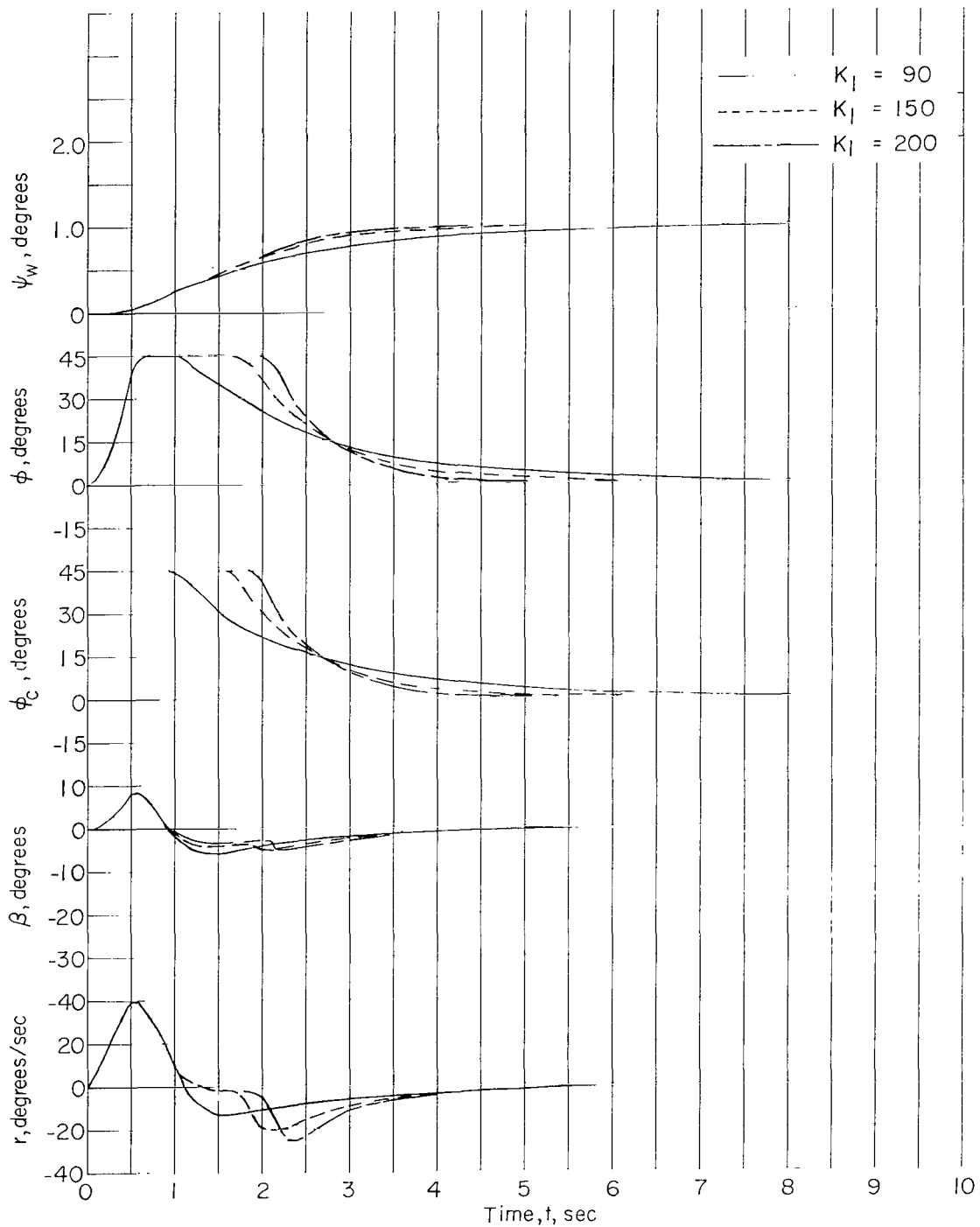
(c) $\psi_{w,c} = 1.00°$.

Figure 8.- Continued.
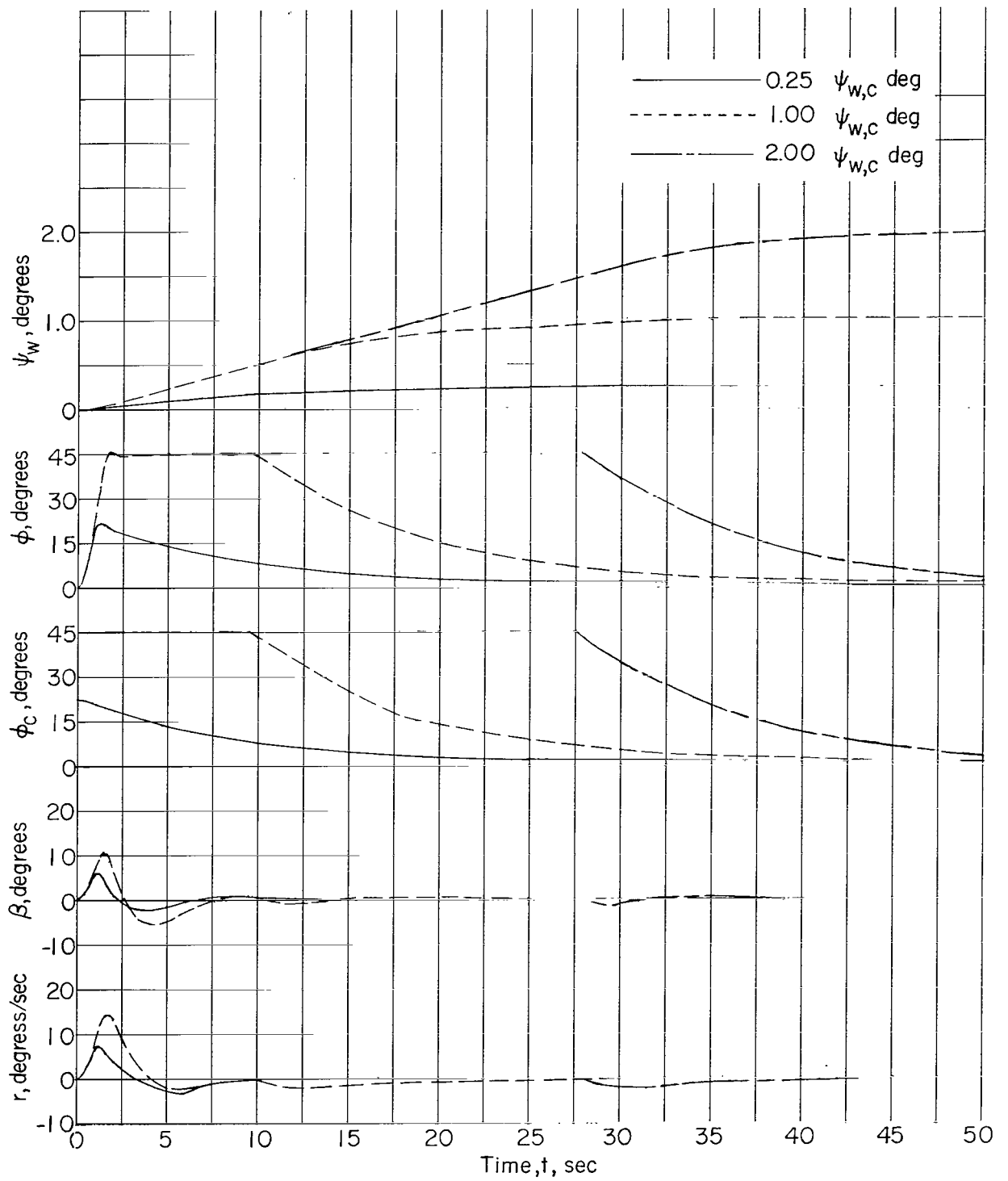
(d) $\psi_{w,c} = 2.00°$.

Figure 8.- Concluded.

Figure 9.- Effect of command heading angle on vehicle lateral response at 210,000 feet for $K_1 = 90.0$ and with sideslip damper. $K_2 = 50.0$; $K_3 = 23.0$; $K_4 = 6.00$; $K_5 = 3.00$.

"The aeronautical and space activities of the United States shall be conducted so as to contribute . . . to the expansion of human knowledge of phenomena in the atmosphere and space. The Administration shall provide for the widest practicable and appropriate dissemination of information concerning its activities and the results thereof."

—NATIONAL AERONAUTICS AND SPACE ACT OF 1958

NASA SCIENTIFIC AND TECHNICAL PUBLICATIONS

TECHNICAL REPORTS: Scientific and technical information considered important, complete, and a lasting contribution to existing knowledge.

TECHNICAL NOTES: Information less broad in scope but nevertheless of importance as a contribution to existing knowledge.

TECHNICAL MEMORANDUMS: Information receiving limited distribution because of preliminary data, security classification, or other reasons.

CONTRACTOR REPORTS: Technical information generated in connection with a NASA contract or grant and released under NASA auspices.

TECHNICAL TRANSLATIONS: Information published in a foreign language considered to merit NASA distribution in English.

TECHNICAL REPRINTS: Information derived from NASA activities and initially published in the form of journal articles.

SPECIAL PUBLICATIONS: Information derived from or of value to NASA activities but not necessarily reporting the results of individual NASA-programmed scientific efforts. Publications include conference proceedings, monographs, data compilations, handbooks, sourcebooks, and special bibliographies.

Details on the availability of these publications may be obtained from:

SCIENTIFIC AND TECHNICAL INFORMATION DIVISION

NATIONAL AERONAUTICS AND SPACE ADMINISTRATION

Washington, D.C. 20546